Supplemental Information

CD137 promotes bone metastasis of breast cancer by enhancing the migration and osteoclast differentiation of monocytes/macrophages

Pengling Jiang[1,3,4], Wenjuan Gao[2], Tiansi Ma[2], Rongrong Wang[2], Yongjun Piao[2], Xiaoli Dong[2], Peng Wang[2], Xuehui Zhang[3,5], Yanhua Liu[2,6], Weijun Su[2,6], Rong Xiang[2,6], Jin Zhang[1,3,4,*] and Na Li [2,6,*]

From [1]Third Department of Breast Cancer, Tianjin Medical University Cancer Institute and Hospital, National Clinical Research Center for Cancer, Key Laboratory of Cancer Prevention and Therapy, Tianjin, China;
[2]School of Medicine, Nankai University, 94 Weijin Road, Tianjin, China;
[3]Tianjin's Clinical Research Center for Cancer, Tianjin, China;
[4]Key Laboratory of Breast Cancer Prevention and Therapy, Tianjin Medical University, Ministry of Education, Tianjin, China;
[5] Department of Blood Transfusion, Tianjin Medical University Cancer Institute and Hospital, National Clinical Research Center for Cancer, Key Laboratory of Cancer Prevention and Therapy, Tianjin, China;
[6]Tianjin Key Laboratory of Tumour Microenvironment and Neurovascular Regulation, Tianjin, China.

**** Correspondence to: Dr. Jin Zhang, zhangjin@tjmuch.com; Dr. Na Li, lina08@nankai.edu.cn.***

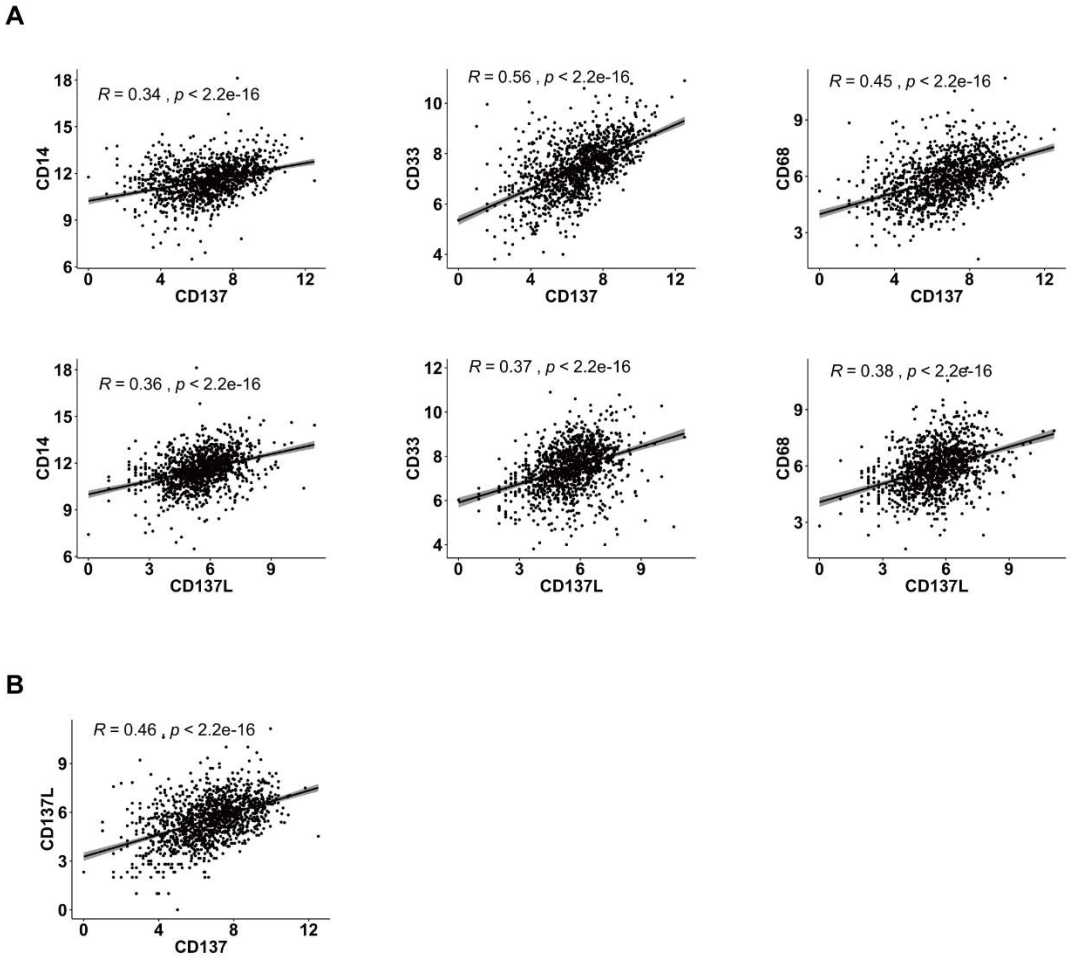

Figure S1. CD137 and CD137L correlate with macrophages markers in human breast cancers. A-B. Pearson's correlation analysis of CD137 and CD137L with macrophage markers (CD14, CD33, CD68) at mRNA level, respectively (**A**) and the correlation between CD137 mRNA and CD137L mRNA (**B**) in the primary human breast cancers of TCGA database.

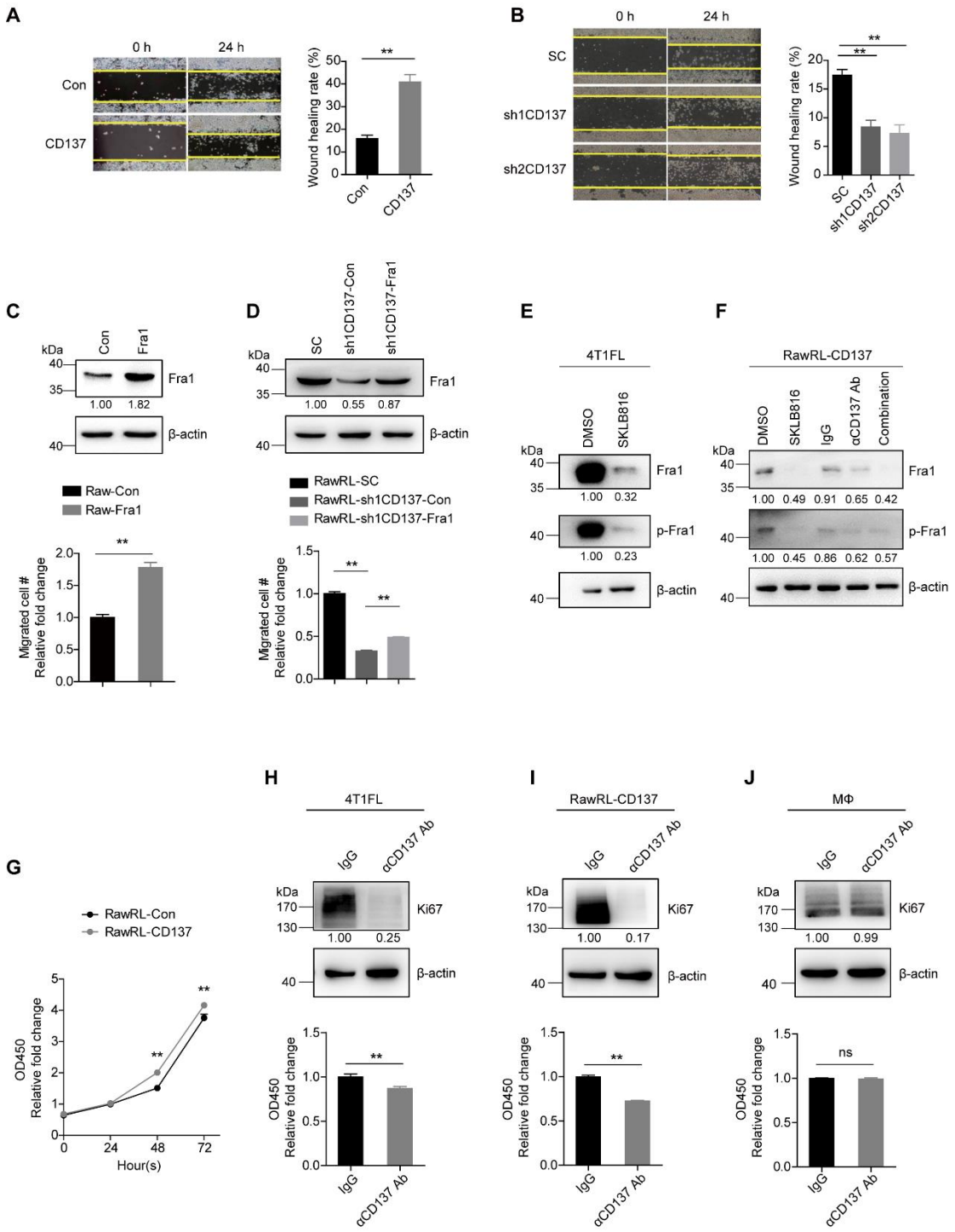

Figure S2. CD137 promotes the migration of monocytes/macrophages through Fra1. A-B. Representative wound healing assay of RawRL cells (Left panel, the edge of the wound was indicated by the yellow line) and the statistical results (right panel, n = 3). **C-D.** Upper panel: Western blot results of Fra1 in RAW264.7 and RawRL cells. The mean value of relative fold change (RFC) for each blot is indicated at the bottom, n = 2. Lower panel: statistical results of the transwell assay in RAW264.7 and RawRL cells (n = 3-6). **E-F.** Western blot results of Fra1 and p-Fra1 in 4T1FL cells treated with DMSO and SKLB816 (**E**) and in RawRL-CD137 cells treated with DMSO, SKLB816, IgG, αCD137 Ab, and SKLB816 combined with αCD137 Ab (combination). The mean RFC value for each blot is indicated at the bottom, n = 3. **G.** Time

dependent CCK8 assay of cell viability change of RawRL after their adhesion to the plate (n = 8). Cell viability of RawRL-Con at 24 hours after the adhesion was used as the control. **H-J.** Western blot results of Ki67 (upper panel, the mean RFC value for each blot is indicated at the bottom, n = 3) and statistical results for CCK8 assay of the cell viability change in 4T1FL, RawRL-CD137 cells and primarily cultured macrophages (MΦ) treated with IgG and αCD137 Ab for 24 hours (lower panel, n = 6-8). Abbreviation: h: hour(s).

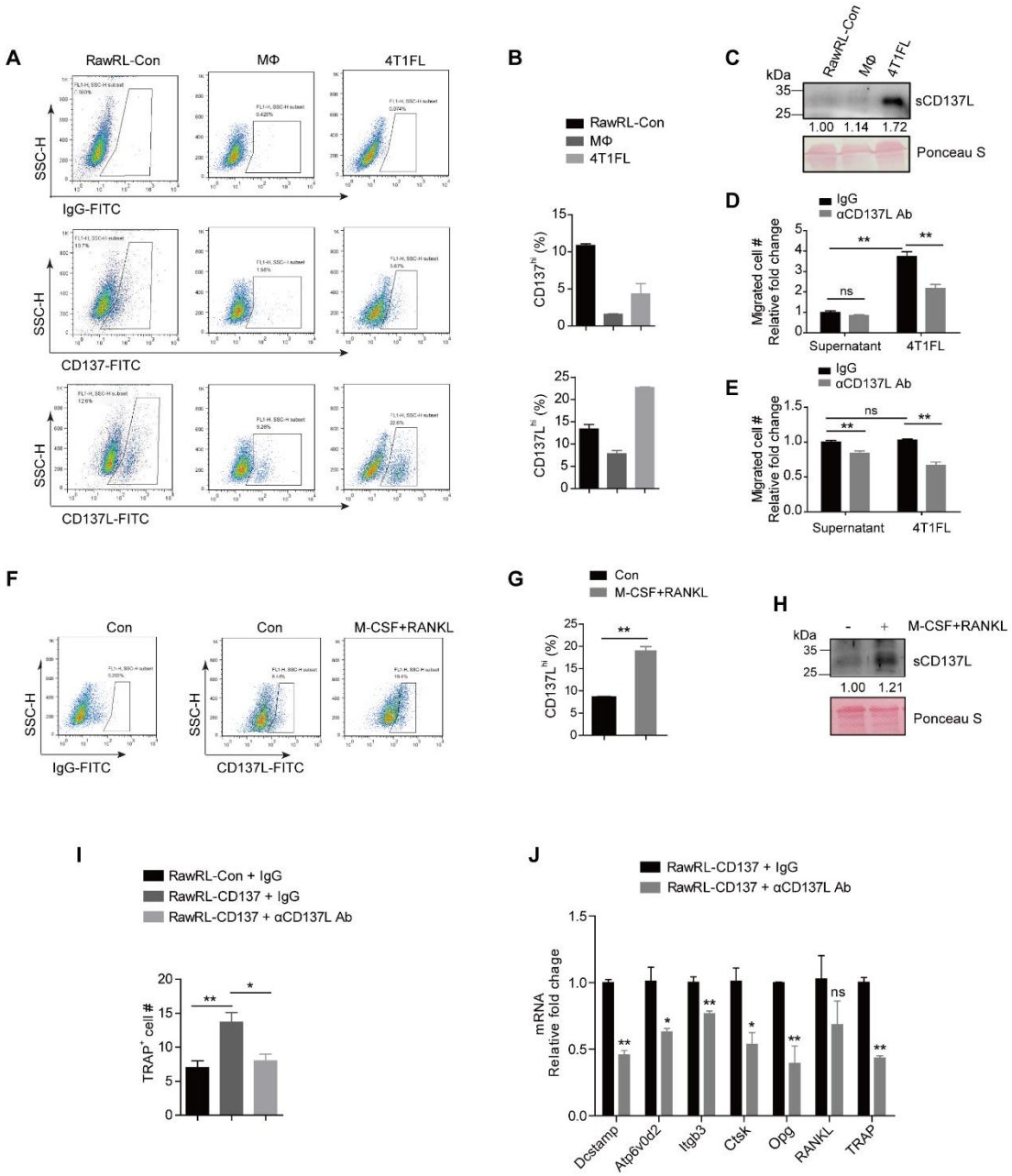

Figure S3. CD137L-CD137 signaling promotes the migration and osteoclast differentiation of monocytes/macrophages. A-B. Representative FACS analysis of membrane-bound CD137^{hi} and CD137L^{hi} cells in RawRL-Con, MΦ and 4T1FL cells (**A**) and the statistical results (n = 3, **B**). **C.** Western blot results of sCD137L in the supernatant of RawRL-Con, MΦ and 4T1FL cells. The mean RFC value for each blot is indicated at the bottom (n = 4). **D-E.** Statistical results of transwell assay of the recruitment of MΦ (**D**) and RawRL-Con (**E**) by 4T1FL cells or their supernatant after application of IgG and αCD137L Ab to the lower chamber (n = 3-4). **F-G.** Representative FACS analysis of membrane bound CD137L^{hi} cells in RawRL-Con cells after incubation with M-CSF (10 ng/mL) and RANKL (100 ng/mL) for 9 days (**F**) and the statistical results (**G**, n = 3). The untreated RawRL-Con cells were used as the control (Con). **H.** Representative Western blot results of sCD137L in the supernatant of RawRL-Con cells after incubation with or without M-CSF (10 ng/mL) and RANKL (100 ng/mL) for 9 days, the mean RFC value for each blot is indicated at the bottom, n = 2. **I.**

Statistical results of the number of $TRAP^+$ osteoclasts in RawRL cells which were treated with M-CSF (10 ng/mL) and RANKL (100 ng/mL) in the presence of 10 μg/mL αCD137L Ab or IgG for 9 days (n = 3). **J.** Real-time PCR assay of relative mRNA level changes of different genes in RawRL-CD137, which were treated with M-CSF (10 ng/mL) and RANKL (100 ng/mL) in the presence of 10 μg/mL αCD137L Ab or IgG for 9 days (n = 3).

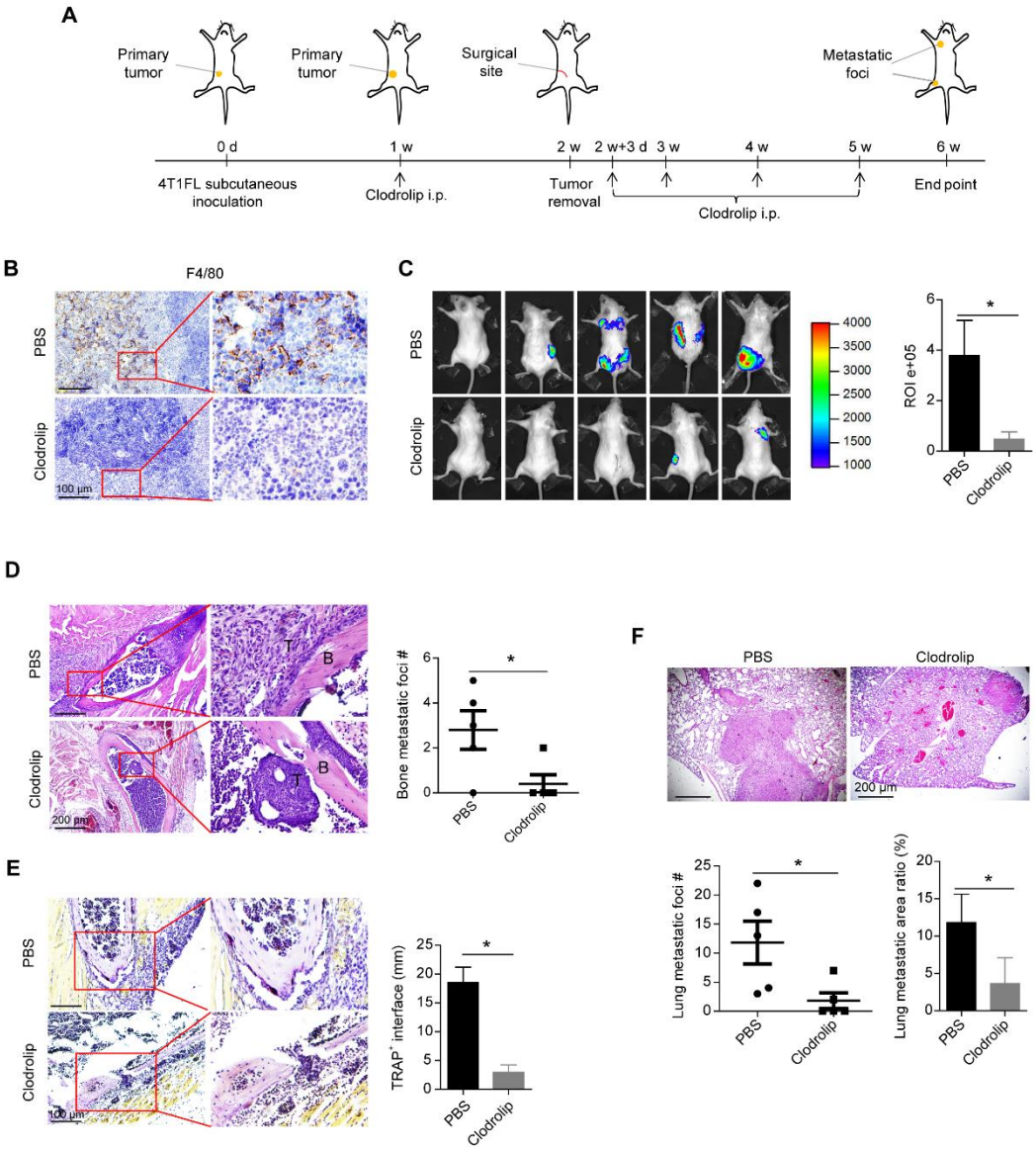

Figure S4. Depletion of monocytes/macrophages by clodrolip inhibits bone metastases of breast cancer. A. Schematic diagram of experiment procedure. Clodrolip or its PBS control was administrated at the time points indicated by arrows. **B.** IHC staining of F4/80 in the spleen from a representative mouse treated with clodrolip or PBS (scale bar: 100 μm). **C.** Left panel: BLI image of tumor-invasion lesions in each mouse at the end point of experiment. Right panel: Statistical results of normalized BLI signals (n = 5 mice). **D.** Left panel: H&E staining image of bone lesion invaded by tumor from a representative mouse in each group (scale bar: 200 μm). Right panel: Statistical results of bone metastatic foci number (#), data are presented as mean ± SEM (n = 5 mice). **E.** Left panel: TRAP staining of the osteolytic bone lesion from a representative mouse in each group (scale bar: 100 μm). Right panel: Statistical results of $TRAP^+$ osteoclasts in osteolytic bone lesions (n = 2-12 bone lesions). **F.** Upper panel: H&E staining image of lung metastasis from a representative mouse in each group (scale bar: 200 μm). Lower panel: Statistical results of lung metastatic foci number (data are presented as mean ± SEM, n=5 mice) and lung metastatic area ratio (n = 5 mice). Abbreviation: i.p.: intraperitoneal injection.

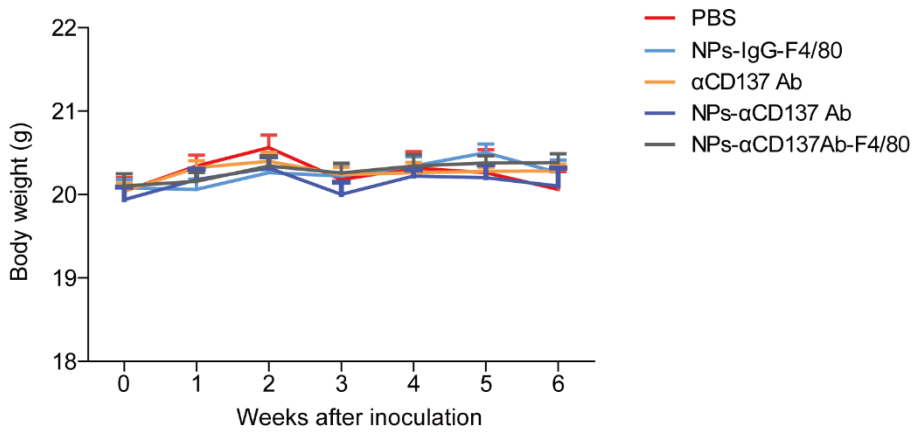

Figure S5. NPs-αCD137 Ab-F4/80 have no obvious effect on the body weight of tumor-bearing BALB/c mice. Statistical results of the body weight of tumor-bearing BALB/c mice receiving NPs-αCD137 Ab-F4/80 treatment and the controls shown in Figure 5, n = 5 mice.

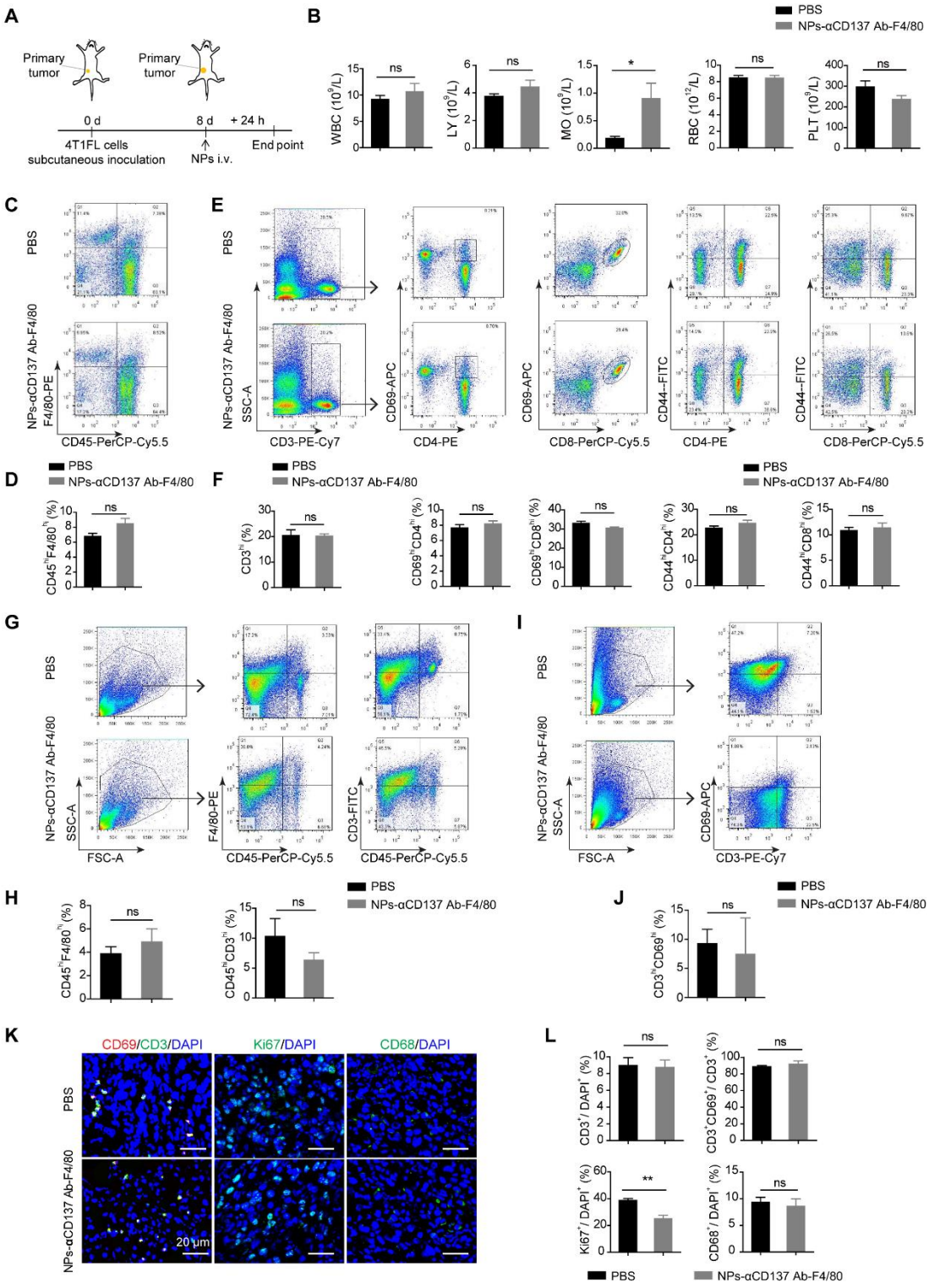

Figure S6. NPs-CD137 Ab-F4/80 have no obvious effect on T cell activation *in vivo*. A. Schematic diagram of experiment procedure. **B.** Statistical results for the hematological assays of tumor-bearing BALB/c mice that were treated with PBS or NPs-αCD137 Ab-F4/80 for 24 hours (n = 5 mice). **C-F.** Representative FACS results of spleen leukocytes (**C, E**) and the statistical results for the percentage of $CD45^{hi}F4/80^{hi}$ cells (**D**), $CD3^{hi}$ cells **(F)** in spleen leukocytes and the percentage of $CD69^{hi}CD4^{hi}$, $CD69^{hi}CD8^{hi}$, $CD44^{hi}CD4^{hi}$ and $CD44^{hi}CD8^{hi}$

cells in the spleen $CD3^{hi}$ cells (**F)** of tumor-bearing BALB/c mice that were treated with PBS or NPs-αCD137 Ab-F4/80 for 24 hours (n = 5 mice)**. G-J.** Representative FACS results (**G, I**) and the statistical results for the percentage of $CD45^{hi}F4/80^{hi}$, $CD45^{hi}CD3^{hi}$ cells (**H**) and $CD3^{hi}CD69^{hi}$ cells (**J**) in 4T1FL-allografts of BALB/c mice that were treated with PBS or NPs-αCD137 Ab-F4/80 for 24 hours (n = 5 mice). **K-L.** Representative confocal images of CD69 (red) and CD3 (green), Ki67 (green) and CD68 (green), scale bar: 20 μm (**K**), and the statistical results for the ratio of $CD3^{+}/DAPI^{+}$, $CD3^{+}CD69^{+}/CD3^{+}$, $Ki67^{+}/DAPI^{+}$ and $CD68^{+}/DAPI^{+}$ cells in 4T1FL-allografts of BALB/c mice that were treated with PBS or NPs-αCD137 Ab-F4/80 for 24 hours, n = 3-5 mice (**L**). Abbreviation: d: day(s); h: hours; i.v.: intravenous injection; WBC: white blood cell; LY: lymphocyte; MO: monocyte; RBC, red blood cell; PLT, platelet.

Table S1. The primers used in real-time PCR assay.

Gene name	Primer
Dcstamp (*Mus*)	Forward: 5'- TACGTGGAGAGAAGCAAGGAA -3'
	Reverse: 5'- ACACTGAGACGTGGTTTAGGAAT -3'
Atp6v0d2 (*Mus*)	Forward: 5'- CAGAGCTGTACTTCAATGTGGAC -3'
	Reverse: 5'- AGGTCTCACACTGCACTAGGT -3'
Itgb3 (*Mus*)	Forward: 5'- CCACACGAGGCGTGAACTC -3'
	Reverse: 5'- CTTCAGGTTACATCGGGGTGA -3'
Ctsk (*Mus*)	Forward: 5'- GAAGAAGACTCACCAGAAGCAG -3'
	Reverse: 5'- TCCAGGTTATGGGCAGAGATT -3'
Opg (*Mus*)	Forward: 5'- ACCCAGAAACTGGTCATCAGC -3'
	Reverse: 5'- CTGCAATACACACACTCATCACT -3'
RANKL (*Mus*)	Forward: 5'- CAGCATCGCTCTGTTCCTGTA -3'
	Reverse: 5'- CTGCGTTTTCATGGAGTCTCA -3'
TRAP (*Mus*)	Forward: 5'- CACTCCCACCCTGAGATTTGT -3'
	Reverse: 5'- CATCGTCTGCACGGTTCTG -3'

Table S2. Clinical characteristics and IHC staining results of CD137 and CD137L in patients with breast carcinoma.

Case number	Gender	Age	Diagnosis	Histological grade	TNM stage	CD137 stain	CD137L stain
1	F	38	Invasive ductal carcinoma	2	IIB	Negative	Positive
2	F	65	Invasive ductal carcinoma	1	IIA	Negative	Negative
3	F	57	Invasive ductal carcinoma	1	IIA	Negative	Positive
4	F	40	Invasive ductal carcinoma	1	IIA	Negative	Negative
5	F	47	Invasive ductal carcinoma	1	IIA	Negative	Positive
6	F	52	Invasive ductal carcinoma	1	IIB	Negative	Negative
7	F	48	Invasive ductal carcinoma	1	IIA	Negative	Negative
8	F	54	Invasive ductal carcinoma	1	IIA	Positive	Negative
9	F	45	Invasive ductal carcinoma	1	IIA	Positive	Negative
10	F	47	Invasive ductal carcinoma	1	IIA	Positive	Positive
11	F	64	Invasive ductal carcinoma	1	IIA	Positive	Positive
12	F	30	Invasive ductal carcinoma	1	IIA	Negative	Positive
13	F	71	Invasive ductal carcinoma	2	IIA	Positive	Positive
14	F	54	Invasive ductal carcinoma	2	IIB	Positive	Positive
15	F	79	Invasive ductal carcinoma	2	IIB	Positive	Positive
16	F	48	Invasive ductal carcinoma	2	IIIB	Positive	Negative
17	F	45	Invasive ductal carcinoma	2	IIA	Negative	Positive
18	F	47	Invasive ductal carcinoma (sparse)	Unknown	IIA	Positive	Positive
19	F	59	Invasive ductal carcinoma	2	IIA	Positive	Negative
20	F	38	Invasive ductal carcinoma	2	IIB	Positive	Negative
21	F	37	Invasive ductal carcinoma	2	IIB	Positive	Positive
22	F	47	Invasive ductal carcinoma	2	IIA	Positive	Positive
23	F	45	Invasive ductal carcinoma	1	IIIB	Positive	Positive
24	F	60	Invasive ductal carcinoma	2	IIIB	Positive	Positive
25	F	49	Invasive ductal carcinoma with necrosis (sparse)	Unknown	IIA	Positive	Positive
26	F	40	Invasive ductal carcinoma	3	IIA	Positive	Positive
27	F	62	Invasive ductal carcinoma	3	IIA	Positive	Positive
28	F	60	Invasive ductal carcinoma	2	IIA	Positive	Positive
29	F	46	Invasive ductal carcinoma	2	IIA	Positive	Negative
30	F	68	Invasive ductal carcinoma	2	IIIB	Positive	Negative
31	F	53	Invasive ductal carcinoma	3	IIA	Positive	Positive
32	F	57	Invasive ductal carcinoma	3	IIA	Positive	Positive
33	F	81	Invasive ductal carcinoma	Unknown	IIB	Negative	Negative
34	F	63	Invasive ductal carcinoma	3	IIA	Positive	Positive
35	F	35	Invasive ductal carcinoma	3	IIB	Negative	Positive
36	F	65	Invasive ductal carcinoma	3	IIB	Positive	Positive

Table S3. Clinical characteristics of healthy female and female patients with breast cancer (BC) in the ELISA assay of serum sCD68.

	Normal (n = 19)	**Non-metastatic BC** (n = 30)	**Metastatic BC** (n = 30)
Age			
26-35	0 (0%)	1 (3.3%)	0 (0%)
36-45	6 (31.6%)	11 (36.7%)	7 (23.3%)
46-55	12 (63.2%)	17 (56.7%)	23 (76.7%)
56-70	0 (0%)	1 (3.3%)	0 (0%)
unknown	1 (5.3%)	0 (0%)	0 (0%)
Metastatic site			
Bone w/wo other sites	NA	NA	16 (53.3%)
other sites (LN(s), chest wall, liver, lung, etc.)	NA	NA	14 (46.7%)

Abbreviation: w/wo: with/without; LN(s): lymph node(s); NA: not applicable.

Table S4. Clinical characteristics of health female and female patients with breast cancer (BC) in the Western blot analysis of serum sCD137L.

	Normal (n = 20)	**Non-metastatic BC** (n = 22)	**Metastatic BC** (n = 22)
Age			
26-35	0 (0%)	2 (9.1%)	0 (0%)
36-45	6 (30%)	9 (40.9%)	11 (50.0%)
46-55	13 (65%)	10 (45.5%)	11 (50.0%)
56-70	0 (0%)	1 (4.5%)	0 (0%)
unknown	1 (5%)	0 (0%)	0 (0%)
Metastatic site			
Bone w/wo other sites	NA	NA	14 (63.6%)
other sites (LN(s), chest wall, liver, lung, etc.)	NA	NA	8 (36.4%)

Abbreviation: w/wo: with/without; LN(s): lymph node(s); NA: not applicable.